Praveen Singh, Munmun Kumari, Amanjit Bal, Radhika Srinivasan and Sujata Ghosh*

Heat shock protein 60 is a disease-associated sialoglycoprotein in human non-small cell lung cancer

https://doi.org/10.1515/hsz-2019-0352
Received August 22, 2019; accepted February 3, 2020

Abstract: The diagnostic and therapeutic potential of *Maackia amurensis* agglutinin (MAA) have been reported in various malignancies. Earlier, we have found that MAA specifically interacted with human non-small cell lung-cancer (NSCLC) cells and induced apoptosis in these cells. The present study was designed to identify *M. amurensis* leukoagglutinin (MAL-I, one of the components of MAA, having the same carbohydrate specificity as MAA) interacting membrane sialoglycoprotein(s) of two subtypes of human NSCLC cell lines. Nine proteins were identified using two-dimensional (2D)-polyacrylamide gel electrophoresis (PAGE) followed by MAL-I-overlay transblotting and matrix assisted laser desorption ionization-time of flight mass spectrometry (MALDI-TOF-MS). Among these proteins, HSP60 was selected for further characterization. The sialoglycoprotein nature of membrane-HSP60 of NSCLC cell lines was confirmed by its reduced reactivity with MAL-I in Western blots in the presence of GM2 and by dual staining of the cell lines with MAL-I and HSP60-antibody. These findings were further substantiated by enzymatic analysis of membrane-HSP60 as well as *in-silico* evidence regarding this protein. Our observations were validated by immunohistochemical analysis of both subtypes of NSCLC tissue sections. Membrane-HSP60 was found to be involved in the inhibition of MAL-I-induced morphological alteration of NSCLC cells and also in the proliferation and migration of these cells, indicating the probable role of sialylated membrane-HSP60 in this disease.

***Corresponding author: Sujata Ghosh,** Department of Experimental Medicine and Biotechnology, PGIMER, Chandigarh 160012, India, e-mail: sujataghosh12@gmail.com. https://orcid.org/0000-0002-8360-0508
Praveen Singh and Munmun Kumari: Department of Experimental Medicine and Biotechnology, PGIMER, Chandigarh 160012, India
Amanjit Bal: Department of Histopathology, PGIMER, Chandigarh 160012, India
Radhika Srinivasan: Department of Cytology and Gynecological Pathology, PGIMER, Chandigarh 160012, India

Keywords: HSP60; lung cancer; *Maackia amurensis* agglutinin; sialoglycoprotein.

Introduction

Lung cancer is one of the major causes of cancer-associated deaths worldwide (Bray et al., 2018). The prevalence of this disease is increasing in developing countries including India (Parikh et al., 2016). Non-small cell lung-cancer (NSCLC), the major sub-type, accounts for ~85% of all lung cancer cases (Oser et al., 2015). Despite the advances in cancer treatment strategies, the prognosis of lung cancer patients has improved nominally. Thus, efforts are going on to develop clinically-useful better treatment strategies for this disease.

Altered glycosylation, specifically sialylation is a hallmark of cancer cells. Aberrant sialylation of cellular glycoconjugates were shown to modulate different cellular processes associated with tumorigenesis (Isaji et al., 2019). Altered sialylation has been detected in various epithelial cancers (Ma et al., 2016; Munkley and Scott, 2019). Neo-expression or overexpression of sialylated epitopes, for example, sialyl-Tn, sialyl-T, sialyl-Le^x and sialyl-Le^a was also noted on the surface of lung cancer cells (Hauselmann and Borsig, 2014). Lectins, the carbohydrate specific biomolecules, have been used to predict such altered patterns of glycosylation in cancer (Singh et al., 2019). Studies have revealed the diagnostic potential of various lectins in cancer of different origins (Syed et al., 2016; Silva, 2018; Pearson and Gallagher, 2019). Further, several lectins were shown to have anticancer properties (Yau et al., 2015; Ribeiro et al., 2018).

MAA, the potentially important plant agglutinin is known to be a mixture of MAL-I and MAL-II (Kawaguchi et al., 1974; Wang and Cummings, 1988). MAA and MAL-I have specificity for Neu5Acα2,3Galβ1,4GlcNAc/Glc. MAA revealed diagnostic potential in prostate cancer and cervical cancer (Ohyama et al., 2004; Lopez-Morales et al., 2010). MAL-I also showed diagnostic potential in cancer of papilla of vater, thyroid cancer, colorectal cancer and gastric cancer (Tang et al., 2005; Babal et al., 2006;

Published online March 03, 2020

Inagaki et al., 2007, 2008). In the previous study, we found that MAA could recognize childhood-acute lymphoblastic leukemic-cells and activate the mitochondrial apoptotic pathway in these cells (Kapoor et al., 2008). We also demonstrated strong reactivity of this agglutinin with the NSCLC cells and found that it could interact with a membrane-glycoprotein band (M_r ~ 66 kDa) of NSCLC cell lines (Mehta et al., 2010). Furthermore, we observed the apoptotic activity of MAA in these cells as well as in the drug-resistant NSCLC sublines (Mehta et al., 2013; Lalli et al., 2019). We also reported the chemoadjuvant potential of this agglutinin in NSCLC (Lalli et al., 2015). Moreover, Ochoa-Alvarez et al. (2012) found that this agglutinin could inhibit tumor cell growth and its migration in a mouse model of melanoma. All this evidence clearly indicated the possible therapeutic potential of MAA in cancer of different origins.

Aberrant sialylation of cell surface glycoproteins has also been found to be related to the poor prognosis of various malignancies (Munkley and Scott, 2019). Thus, exploration of disease-associated sialoglycoproteins and study on their role in the disease progression is a relevant approach to gain a deeper insight into the disease pathogenesis. However, the MAA/MAL-I interacting membrane-glycoprotein(s) of NSCLC cells of different subtypes have not been identified so far. Thus, the aim of this study was to identify MAL-I interacting membrane-sialoglycoprotein(s) of the two major subtypes of NSCLC cell lines.

Results

NSCLC cell lines

The photomicrographs of two major subtypes of NSCLC cell lines are shown in Figure 1. In all the experiments, exponentially growing cultures were used. The average yield of the membrane proteins (Adamo et al., 1992) of A549 and NCI-H520 cells was 2.27 mg and 2.12 mg, respectively.

MAL-I interacts with the membrane proteins of NSCLC cell lines

A significantly high reactivity of MAL-I with the membrane fraction of each cell type (A549: 11.9-fold; NCI-H520: 6.5-fold) was noted, as assessed by an MAL-I overlay enzyme linked assay (Figure 2A). The representative two-dimensional (2D)-polyacrylamide gel electrophoresis (PAGE) profiles of the membrane proteins of NSCLC cell lines are shown in Figure 2B (I and V). Several MAL-I interacting proteins in the respective representative transblots were found to be highlighted in the molecular weight (M_r) range of 20–100 kDa and the isoelectric point (pI) range of 4.5–6.8, as depicted in Figure 2B (II and VI). Furthermore, the membrane proteins of each subtype of the NSCLC cell line were enriched using a Mem-PER™ Kit, the yield of the proteins in each case was ~100 µg. Figure 2B (III and VII) shows the representative profile of the membrane proteins of each cell line in 2D-PAGE. MAL-I interacting proteins in the respective transblots (representative) are depicted in Figure 2B (IV and VIII). Table 1 reveals that several highlighted proteins of each cell line were identical to those, obtained earlier in the case of the membrane proteins prepared by the method of Adamo et al. (1992).

MAL-I interacting membrane proteins of NSCLC cell lines have been identified by MALDI-TOF-MS

MAL-I interacting all the membrane proteins, as indicated in Figure 2B, were selected for matrix assisted laser desorption ionization-time of flight mass spectrometry (MALDI-TOF-MS) analysis. Table 2 reveals the result of the analysis of each spot in view of the name of each most probable identified protein along with pI, M_r, Mowse score, sequence coverage and number of peptides matched, respectively, as obtained from MSDB database. These probable proteins were glucose-regulated protein 78 [GRP78 (GRP78_HUMAN)], 60 kDa heat shock protein [HSP60 (CH60_HUMAN)], actin, cytoplasmic 1 (ACTB_HUMAN), prohibitin (PHB_HUMAN) and heat shock cognate protein 71 kDa (HSP 71) in the case of A549 cells. Whereas endoplasmin (ENPL_HUMAN), HSP-60 (60 kDa heat shock protein), actin, cytoplasmic 1 (ACTB_HUMAN), tubulin alpha 1A chain (TBA1A_HUMAN), alpha enolase (ENOA_HUMAN) and protein disulfide isomerase A3 (PDIA3_HUMAN) were found in the case of NCI-H520. Among these proteins, HSP60 and actin, cytoplasmic 1 were common in the case of both the NSCLC cell lines. HSP60 was selected for further study because of its importance in human cancer of different origins. The representative peptide mass fingerprint (PMF) profile of HSP-60 is shown in Figure 3A. Subsequent MS analysis of each selected peptide ion of HSP-60 was done to obtain the peptide sequence tag, which was used to substantiate the identification of this protein (Figure 3B). This identified protein was

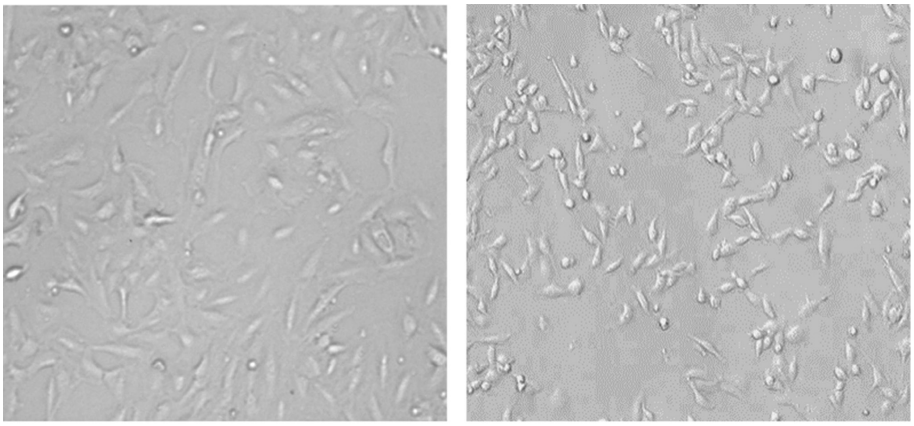

Figure 1: Photomicrographs of A549 and NCI-H520 cell lines under light microscope.
Original magnification was 100×.

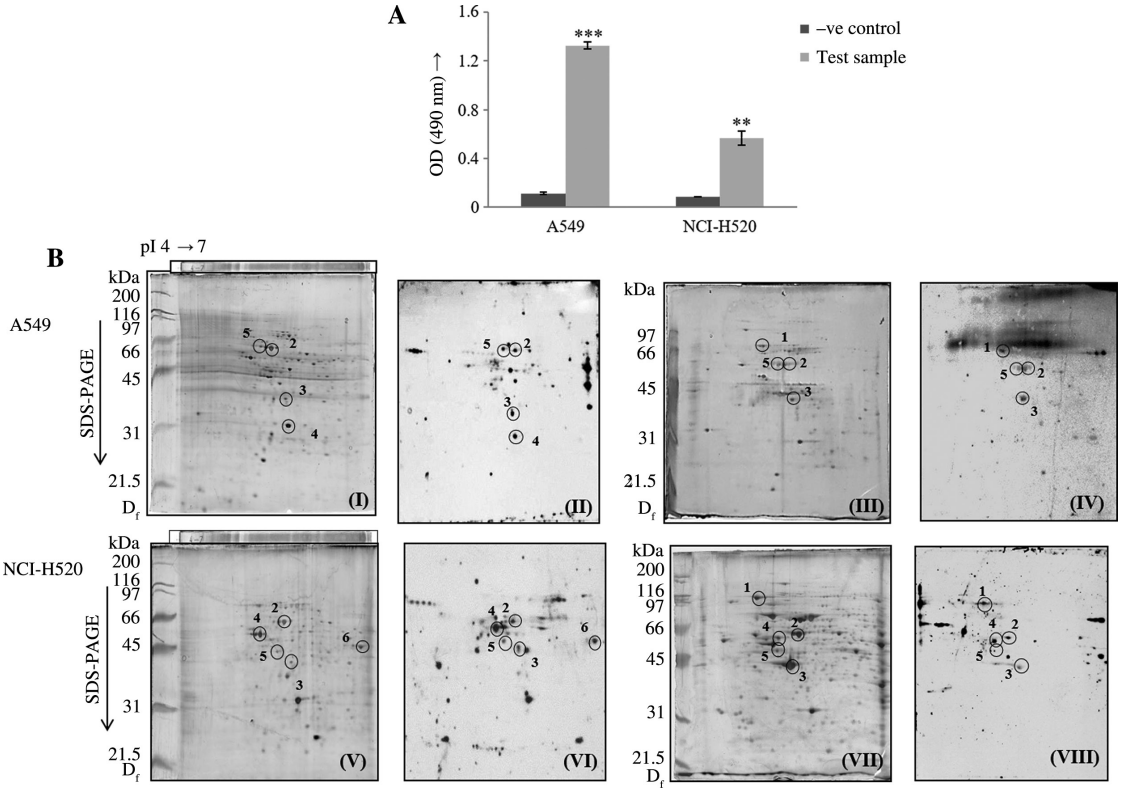

Figure 2: Assessment of the reactivity of MAL-I with the membrane fractions of NSCLC cell lines.
(A) Lectin overlay-Enzyme linked assay; (B) Lectin overlay-Trans blotting. 2D-PAGE profile of the membrane proteins isolated by the method of Adamo et al. (1992) [(I): A549 cells and (V): NCI-H520] and by using Mem-PER™ Eukaryotic protein extraction reagent kit [(III): A549 cells and (VII): NCI-H520]; the respective MAL-I overlay-trans blots [(II): A549 cells and (VI): NCI-H520; (IV): A549 cells and (VIII): NCI-H520]. The M_r and the pI of the proteins of interest were determined from the plot of relative electrophoretic mobility (R_f) of the markers against their respective M_r and the plot of pI of the markers against their respective distance from the anode, respectively.

confirmed as HSP60 by Western immunoblotting using a commercially available antibody (Table 3) against HSP60, which could detect the band of M_r ~66 kDa, present in the membrane fractions of both the NSCLC cell lines following sodium dodecyl sulfate (SDS)-PAGE (Figure 4A, lane 1).

Table 1: Detection of MAL-I interacting membrane proteins of NSCLC cell lines.

Spot No.	Spots (pI and M_r) detected in trans-blots following 2D-PAGE of membrane proteins isolated by			
	Adamo et al. (1992) – method		Mem-PER™ Eukaryotic protein extraction reagent kit	
	A549 cells	NCI-H520 cells	A549 cells	NCI-H520 cells
1	–	–	5.1; 71.5 kDa	4.95; 100 kDa
2	5.5; 64.5 kDa	5.6; 65 kDa	5.5; 62.5 kDa	5.55; 64.5 kDa
3	5.7; 42.5 kDa	5.7; 43.65 kDa	56; 42.75 kDa	5.5; 43.65 kDa
4	5.75; 31.5 kDa	5.3; 55.5 kDa	–	5.3; 58.88 kDa
5	5.3; 65 kDa	5.5; 44.5 kDa	5.4; 62.5 kDa	5.3; 46.46 kDa
6	–	6.65; 43.65 kDa	–	–

Table 2: Identification of MAL-I interacting most probable membrane proteins of NSCLC cell lines by MALDI-TOF-MS analysis.

Spot No.	A549 Cell line	NCI-H520 cell line
1.	Glucose regulated protein 78 (GRP78_HUMAN) Mowse score: 68 Sequence coverage:25%; Peptide match: 14 pI: 5.07; M_r: 72.402 kDa	Endoplasmin (ENPL_HUMAN) Mowse Score: 118 Sequence coverage:31%; Peptide match: 25 pI: 4.76; M_r: 92.696 kDa
2.	Heat shock protein 60 (CH60_HUMAN) Mowse score: 63 Sequence coverage:19%; Peptide match: 11 pI: 5.7; M_r: 61.055 kDa	Heat shock protein 60 (CH60_HUMAN) Mowse score: 253 Sequence coverage:56%; Peptide match: 33 pI: 5.7; M_r: 61.055 kDa
3.	Actin, cytoplasmic 1 (ACTB_HUMAN) Mowse score: 62 Sequence coverage:29%; Peptide match: 7 pI: 5.3; M_r: 42.052 kDa	Actin, cytoplasmic 1 (ACTB_HUMAN) Mowse score: 82 Sequence coverage:49%; Peptide match: 12 pI: 5.3; M_r: 42.052 kDa
4.	Prohibitin (PHB_HUMAN) Mowse score: 90 Sequence coverage:34%; Peptide match: 9 pI: 5.57; M_r: 29.843 kDa	Tubulin alpha 1A chain (TBA1A_HUMAN) Mowse score: 85 Sequence coverage:35%; Peptide match:13 pI: 4.95; M_r: 50.804 kDa
5.	Heat shock cognate-71kDa (HSP7C_HUMAN); Mowse score: 63 Sequence coverage:56%; Peptide match: 13 pI: 5.01; M_r: 71.082 kDa	Protein disulfide isomerase A6 (PDIA6_HUMAN) Mowse score: 27 Sequence coverage:9%; Peptide match: 3 pI: 4.95; M_r: 48.490 kDa
6.	–	Alpha enolase (ENOA_HUMA) Mowse score: 23 Sequence coverage:11%; Peptide match: 6 pI: 6.99; M_r: 47.038 kDa

HSP60 is a MAL-I interacting membrane-sialoglycoprotein of NSCLC cell lines

We observed that the antibody against HSP60 interacted with the same band of M_r ~ 66 kDa, to which MAL-I interacted (Figure 4A, lane 2). The reactivity of MAL-I to membrane-HSP60 (mHSP60) was inhibited in the presence of GM2 [an inhibitor of MAA (Kapoor et al., 2008/MAL-I)] in the case of both the cell lines (Figure 4A, lane 3), indicating the presence of GM2 type sialylated oligosaccharide(s) in mHSP60 of the NSCLC cell lines. Moreover, it was seen that the intensity of MAL-I interacting mHSP60 band was reduced by ~65% and ~90%, following treatment of the membrane proteins of A549 and NCI-H520 cells, respectively, with neuraminidase (Figure 4A, lane 4; Figure 4B), confirming it to be a sialoglycoprotein in nature. Further, an appreciable reduction in the band intensity of mHSP60 was noted in case of O-glycanase (Figure 4A, lane 5; A549: ~99%, NCI-H520: ~92%) as well as N-glycanase treatment (Figure 4A, lane 6; A549: ~79%, NCI-H520: ~85%) of the membrane proteins, as is also reflected in the bar graphs (Figure 4B). The sialoglycoprotein nature of mHSP60 was substantiated by fluorescence-based dual staining of both subtypes of NSCLC cell lines (Figure 5A).

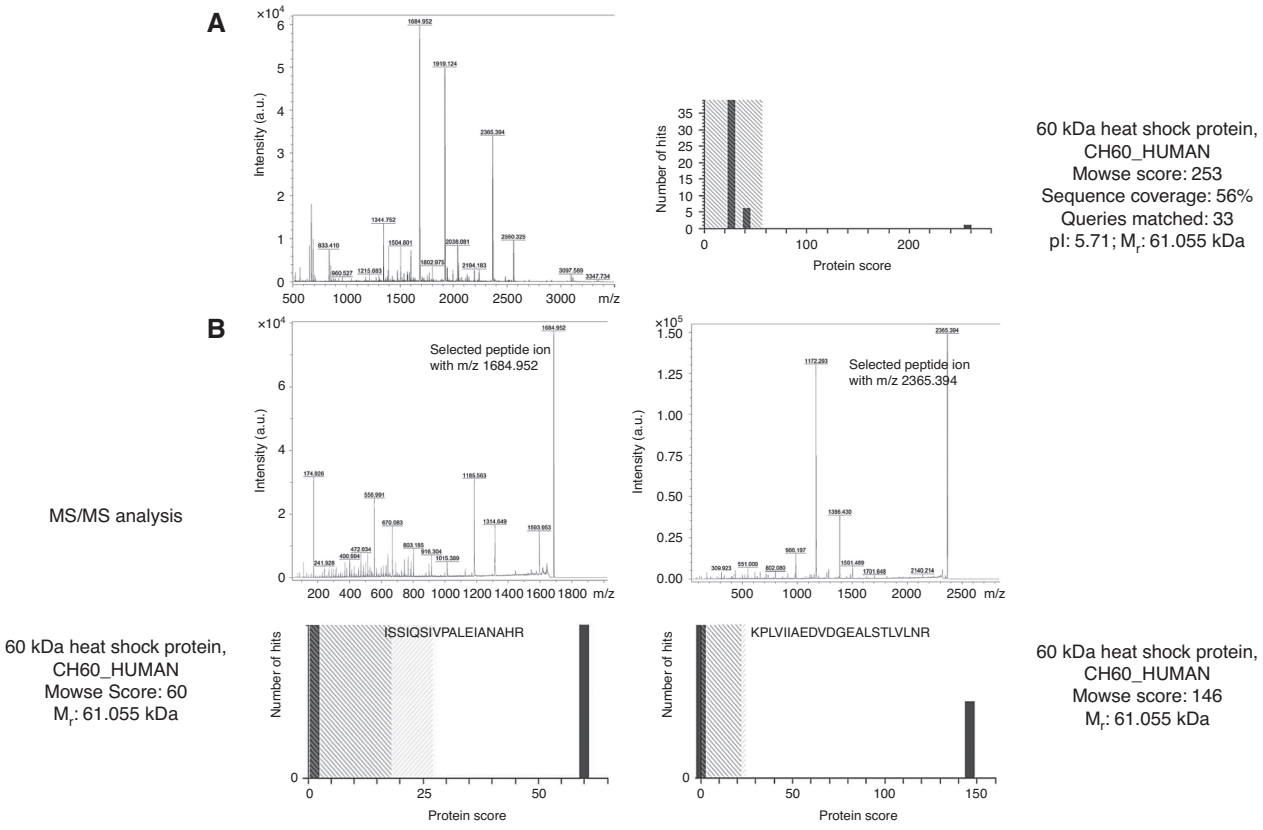

Figure 3: MALDI-TOF-MS analysis.
(A) Representative PMF of spot no. 2 in the case of NCI-H520 cell line along with the respective Mowse score, sequence coverage, number of peptide matched, pI and M_r of the identified protein as obtained from MSDB database using Mascot search engine (Matrix Sciences); (B) MS-MS analysis of the selected peptide ions.

Table 3: Antibody against HSP-60 used in different experiments.

Experiments	Primary antibody			Secondary antibody		
	Antibody clone	Dilution/ concentration	Incubation time/ temperature	Antibody clone	Dilution	Incubation time/ temperature
Western blotting	PA5-34760	1:1000	2 h/37°C	sc2004	1:15 000	1 h/37°C
Immunocytochemistry	PA5-34760	1:400	overnight/4°C	sc2012	1:100	2 h/37°C
Immunohistochemistry	PA5-34760	1:400	2 h/37°C	sc2004	1:100	1 h/37°C
Morphological alteration	PA5-34760	1:250	24 h/37°C	–	–	–
Cell proliferation assay	B-9; sc271215	10 µg/ml	48 h/37°C	–	–	–
Cell migration assay	PA5-34760	1:250	A549; 72 h/37°C NCI-H520; 12 h/37°C	–	–	–

PA5-34760 was procured from (Thermo Fisher Scientific, Waltham, MA, USA). sc: Santa Cruz.

Prominent membrane positivity was seen in the case of the cells, stained with biotinylated MAL-I [used as primary probe; (I)] as well as the antibody against HSP60 [used as primary antibody (Table 3); (II)]. Merging of the two photomicrographs (III) clearly revealed the co-localization mHSP60 and MAL-I interacting protein, indicating mHSP60 is MAL-I interacting sialoglycoprotein.

HSP60 is present in the tissues of NSCLC patients

The presence of HSP60 in tissue sections of lung adenocarcinoma patients (n = 8) and squamous cell carcinoma patients (n = 6) patients was assessed by immunohistochemical analysis using antibody against

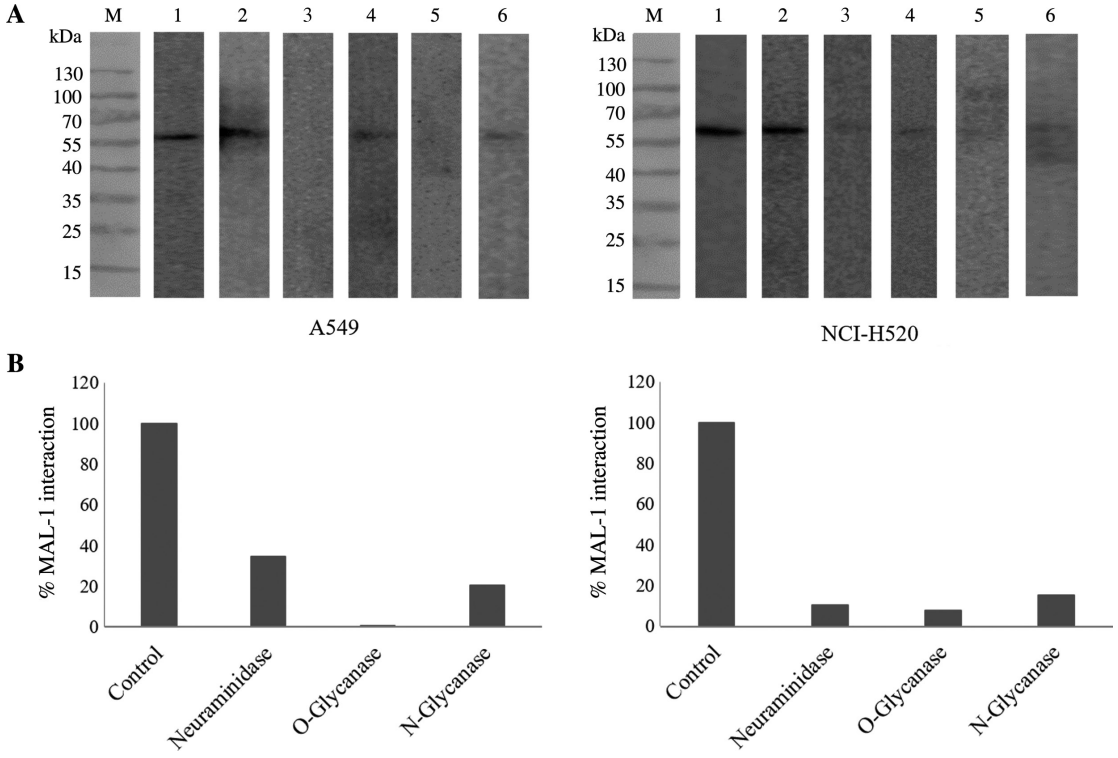

Figure 4: Western blot analysis.
(A) Confirmation of the presence of HSP-60 in membrane fractions of NSCLC cell lines by Western immunoblotting using antibody against HSP-60 (lane 1). Characterization of mHSP60 of NSCLC cell lines as a MAL-1 interacting sialoglycoprotein. Interaction of HSP-60 with MAL-1 in absence (lane 2) and in the presence of GM2 (lane 3). Interaction of MAL-1 with the membrane proteins pre-treated with neuraminidase (lane 4), O-glycanase (lane 5) and N-glycanase (lane 6) on the trans blots. M: molecular weight markers. (B) The bar graphs indicating the intensity of mHSP60 before and after treatment of the membrane proteins with neuraminidase, O-glycanase and N-glycanase separately, as analyzed using ImageJ software.

HSP60 (Table 3) as the primary probe. The representative photomicrographs revealed membrane as well as cytosolic positivity in the case of both types of NSCLC tissue sections, but negligible reactivity with the adjacent normal lung tissue sections (Figure 5B). The H-score (which takes into account the percent positivity and the intensity) ranged from 0 to 300. A significant (*$p < 0.05$) difference in the extent of immunoreactivity between squamous cell carcinoma sections (P) and adenocarcinoma sections (Q) was noted, as obtained by H-score analysis (Figure 5C).

Membrane-HSP60 has functional role in NSCLC cell lines

The antibody against HSP60 (Table 3) was found to inhibit MAL-I induced morphological alteration in both subtypes of NSCLC cell lines (Figure 6A). A reduction (***$p < 0.001$) in the proliferation of A549 cells (2.9-fold) and NCI-H520 cells (1.7-fold) was observed in the presence of HSP60-antibody at 48 h in comparison to the respective control cells (Figure 6B). Analysis of the data of the migration assays revealed that in presence of HSP60-antibody (Table 3), the extent of migration was significantly reduced by 1.3-fold and 1.6-fold in the case of A549 cells and NCI-H520 cells, respectively, as compared to that of the respective controls (Figure 6C).

Discussion

Earlier studies have demonstrated the diagnostic and prognostic potential of *M. amurensis* agglutinin and *M. amurensis* leukoagglutinin (one of the pure components of MAA) in cancers of different origins (Ohyama et al., 2004; Tang et al., 2005; Babal et al., 2006; Inagaki et al., 2007, 2008; Kapoor et al., 2008; Lopez-Morales et al., 2010; Mehta et al., 2010, 2013; Lalli et al., 2015, 2019). Except for podoplanin, no other *M. amurensis* seed lectin interacting protein of cancer cells has been reported to date. In the present study, we have identified the MAA/MAL-I interacting proteins of A549 and NCI-H520 cells, the two

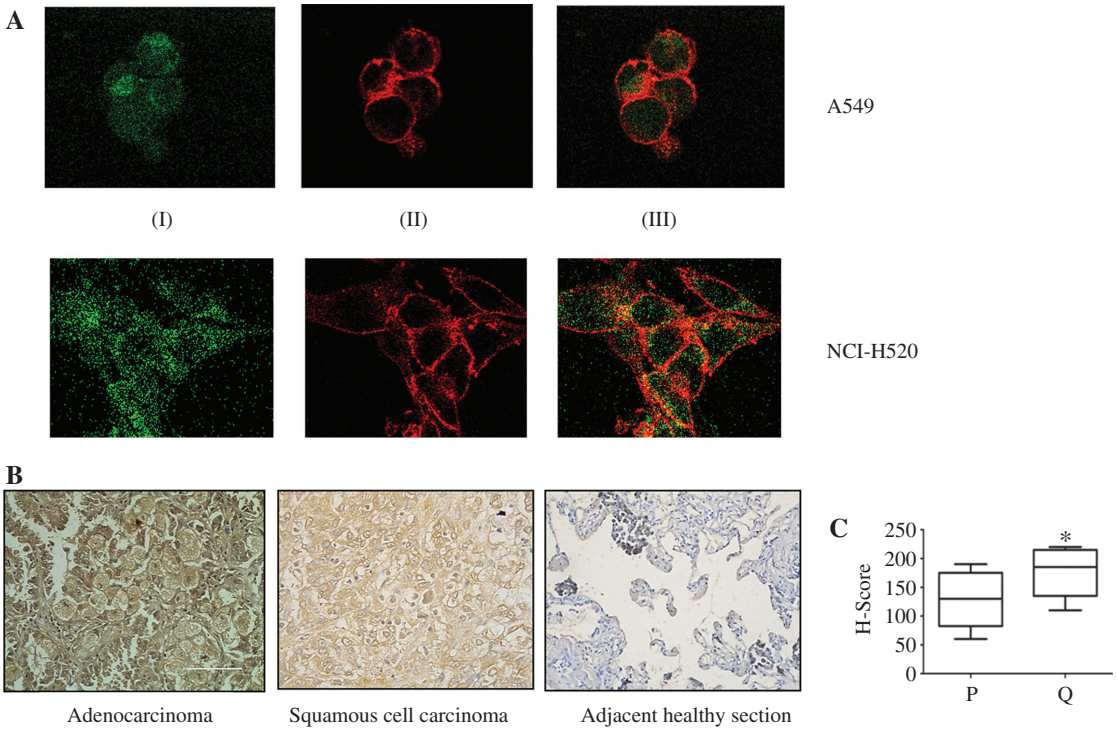

Figure 5: Fluorescence based dual staining of NSCLC cell lines and immunohistochemistry.
(A) Interaction of the cells with (I) HSP-60-Ab and FITC conjugated goat anti-rabbit IgG; (II) Biotinylated MAL-1 and Texas red conjugated streptavidin; (III) merged I and II (original magnification 1000 ×). (B) Representative photomicrographs showing the Interaction of HSP-60-Antibody with the tissue sections of lung adenocarcinoma patient, squamous cell carcinoma patient and adjacent healthy tissue section (original magnification is 100 ×; white scale bar represents 400 μm). (C) H score analysis using GraphPad Prism 6.0. P: Squamous cell carcinoma and Q: adenocarcinoma; *$p < 0.05$ (Q vs. P).

major subtypes of human NSCLC cell lines. As both MAL-I and MAA are specific for Neu5Acα2,3Galβ1,4GlcNAc/Glc, the biotinylated MAL-I was used as a probe for the *in vitro* experiments. Using a glycoproteomic approach based on 2D-PAGE followed by MAL-I-overlay transblotting, several MAL-I interacting proteins of both the NSCLC cell lines were detected. Nine proteins were identified using a Mascot search following MALDI-TOF-tandem mass spectrometric (MS/MS) analysis. All these proteins are known to be related with cancer of different origins.

Endoplasmin (HSP90B1) is a glycoprotein (also known as GRP 94), which is known to be located in the endoplasmic reticulum (ER) of cells (Morales et al., 2009; Marzec et al., 2012). Overexpression of endoplasmin in human lung cancer tissues was found to be related to the differentiation and progression of cancer (Wang et al., 2005). High expression of HSP90B1 in breast cancer tissues was shown to be associated with metastasis and decreased survival (Cawthorn et al., 2012). Hou et al. (2015) observed that high expression of plasma membrane endoplasmin could enhance the invasion and metastatic potential of liver cancer. Actin, cytoplasmic 1, a cytoskeletal glycoprotein was found to be overexpressed in the tissue biopsies of cervical cancer and NSCLC patients (Linxweiler et al., 2014). The abnormal expression and polymerization of this protein and the resulting changes in the cytoskeleton were correlated to the invasiveness and metastasis of cancer (Izdebska et al., 2018). Tubulin alpha 1A is a cytoskeletal protein, found to be localized in the cytoplasm. Expression of this protein was shown to be associated with rectal cancer development (Giarnieri et al., 2005). Protein disulfide isomerase A6 is an enzyme in the ER. Studies have shown that expression of this enzyme on the cell surface could be related to the invasive properties of malignant glioma (Goplen et al., 2006). It has been reported that protein disulfide isomerase A6 could mediate resistance to cisplatin-induced cell death in lung adenocarcinoma (Tufo et al., 2014). Glucose regulated protein 78 (GRP78) has been found to be present in ER, plasma membrane, cytoplasm, mitochondria, nucleus as well as cellular secretions. The presence of this protein on the cell surface led to increased proliferation and migration in breast cancer (Yao et al., 2015). Overexpression of this protein

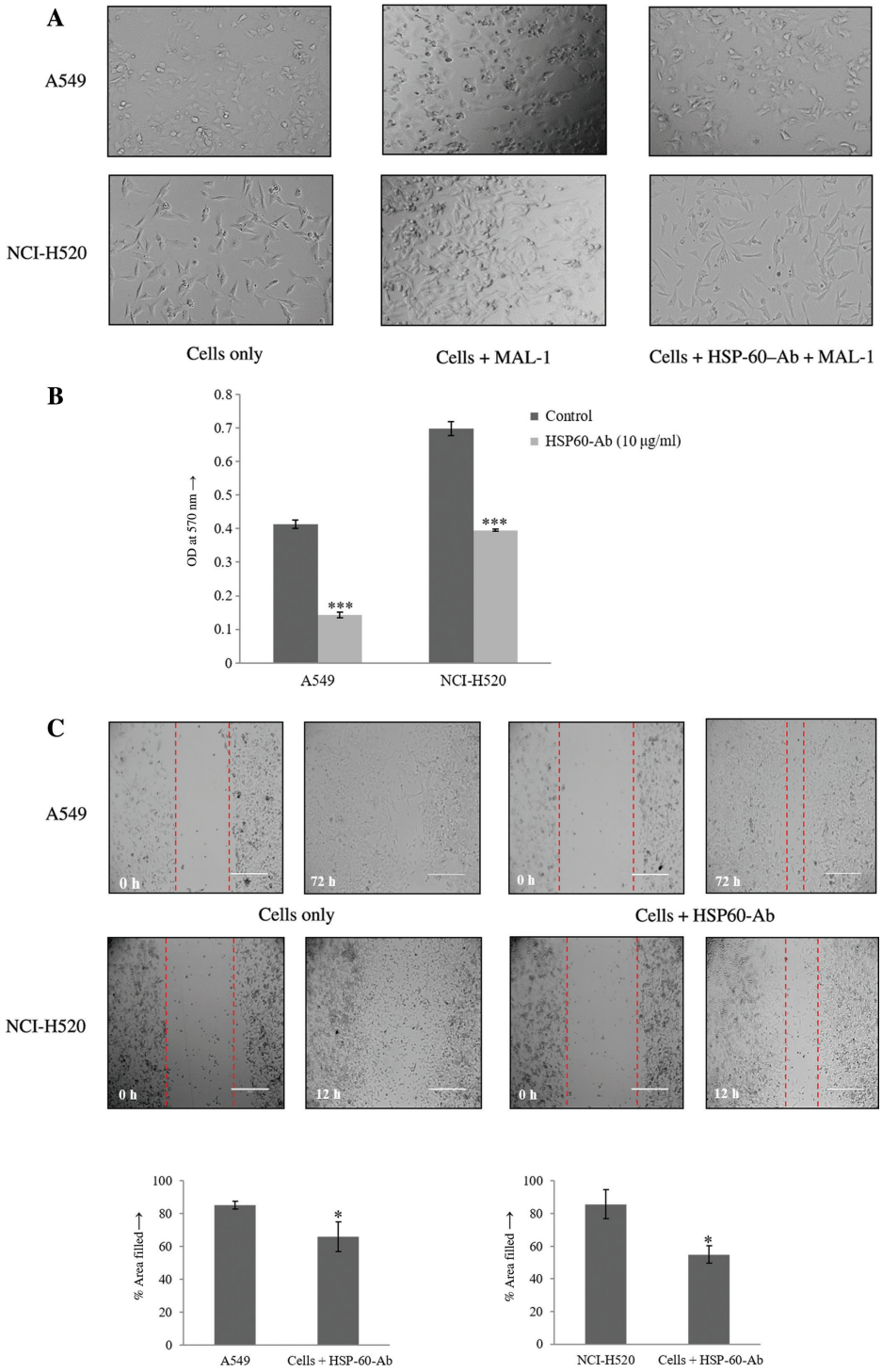

Figure 6: Functional role of mHSP60 in NSCLC cell lines.
Inhibition of (A) MAL-I induced morphological alteration, (B) proliferation and (C) migration of A549 and NCI-H520 cell lines in presence of HSP60-antibody (Ab). Original magnification is 100×; white scale bars represent 400 µm.

was observed in lung cancer, pancreatic cancer and colon cancer that makes this protein an attractive candidate to be used for prognostic implications (Patel et al., 2008). Alpha enolase is a crucial glycolytic enzyme, it was found to be over-expressed in the case of pancreatic cancer (Sun et al., 2017). Furthermore, an increased expression of this protein was shown to be responsible for proliferation and metastasis in the case of NSCLC (Linxweiler et al.,

2014). Prohibitin (PHB) is an evolutionarily conserved pleiotropic protein, located on the cell membrane, inner mitochondrial membrane and nucleus (Xu et al., 2019). High expression of PHB was observed in various cancers, including NSCLC, pancreatic ductal adenocarcinoma and gallbladder cancer (Luan et al., 2014; Zhu et al., 2015; Cao et al., 2016). This protein was found to be involved in the proliferation and dedifferentiation of tumor cells in the case of neuroblastoma (MacArthur et al., 2019). Heat shock cognate 71 (HSC71) kDa protein is known to be expressed in cytoplasm, the endomembrane system and the nucleus. Matsuda et al. (2015) reported that stemness, cell growth and invasion in glioblastoma cells could be regulated by nestin through the alteration of HSC71. Overexpression of this protein was noted in the case of liver cancer and lung cancer (Takashima et al., 2003; Linxweiler et al., 2014). HSP60, the mammalian molecular chaperone, has a crucial role in protein homeostasis via regulating protein folding and assembly (Okamoto et al., 2017). The level of HSP60 was found to be increased in ovarian cancer, androgen-independent locally advanced prostate cancer and lung cancer, in which its presence was detected intracellularly, pericellularly and also in circulation (Castilla et al., 2010; Bodzek et al., 2014; Agababaoglu et al., 2017). Cytosolic HSP60 was shown to have a prognostic association with cervical cancer and colorectal cancer (Cappello et al., 2009; Hwang et al., 2009). The diagnostic and prognostic potential of overexpressed HSP60 was suggested in ovarian, liver, gastric, head and neck and breast cancers (Desmetz et al., 2008; Giaginis et al., 2009; Tsai et al., 2009; Abdalla et al., 2012; Hjerpe et al., 2013). Further, the presence of a high level of serum HSP60 antibodies has been shown to be appreciably associated with the tumor grade of the patients with breast carcinoma (Hamrita et al., 2008). HSP60 was shown to play a vital role in transformation, angiogenesis and metastasis of tumor cells involving the activation of an anti-apoptotic pathway (Wu et al., 2017). Tsai et al. (2009) reported that the activation of β-catenin due to overexpression of HSP60 might indicate a strong propensity towards the tumorigenesis and metastasis in certain tumors. The mechanism underlying the export of HSP60 to the extracellular space and the circulation involves the participation of exosomes, lipid rafts and the classical ER/Golgi protein secretory pathway (Merendino et al., 2010). The presence of HSP60, detected on the surface of Chinese hamster ovary cells, Daudi Burkitt's lymphoma cells and aortic endothelial cells raised the possibility that this chaperonin might also serve as a receptor (Khan et al., 1998). Kamath et al. (2015) suggested the probable involvement of HSP60, induced by EGFR mutants in lung tumor progression. Furthermore, the pro-survival and pro-proliferative activity of HSP60 was noted in neuroblastoma cells (Chaiwatanasirikul and Sala, 2011). However, the role of membrane associated HSP60 (mHSP60) in cancers, including lung cancer has not been reported to date.

The presence of HSP60 was reported in the plasma membrane fraction of human lung adenocarcinoma cells and human lung mucoepidermoid cells but not in the normal human bronchial epithelial cells (Campanella et al., 2012). In this study, we have also found the presence of mHSP60 in the case of the lung squamous cell carcinoma cell line (NCI-H520) along with the adenocarcinoma cell line (A549). We have observed reduced reactivity of MAL-I with mHSP60 on the transblots following O-glycanase as well as N-glycanase treatment, which clearly indicated the presence of both O-and N-linked oligosaccharides in this protein. HSP60 was also found to be post-translationally modified by N-glycosylation in human fibrosarcoma tumor cells. It was proposed that HSP60 might be transported through the ER/Golgi protein secretory pathway in malignant cells, where it could acquire N-glycans and thus could affect the immunological properties of the proteins in the tumor microenvironment (Hayoun et al., 2012). Our observation was in agreement with the *in silico* prediction of the potentially glycosylated sites in HSP-60 protein sequence using GlycoEP software (Chauhan et al., 2013), which revealed the presence of three N-linked glycosylation sites at position 103, 230 and 426 (confidence score > 0.5) as well as seven O-linked glycosylation sites at positions 6, 54, 74, 113, 115, 117 and 547 (confidence score > 0.1).

Binding of lectin to the glycoprotein in the presence of specific inhibitor, is a method that has widely been used to confirm the specific glycan-mediated binding of the lectin (Cummings et al., 2015). In the present study, inhibition of reactivity of MAL-I with mHSP60 on transblots in the presence of GM2 [an inhibitor of MAA (Kapoor et al., 2008)/MAL-I], clearly indicated the presence of Neu5Acα2,3Galβ1,4GlcNAc/Glc in the oligosaccharide portion of mHSP60. We have used commercially available neuraminidase (Sigma-Aldrich, St. Louis, MO, USA), isolated from *Clostridium perfringens*, which is known to hydrolyze terminal N-acetyl-neuraminic acid (sialic acid) residues which are α2,3-, α2,6- or α2,8-linked (rate of hydrolysis: α2,3 > α2,6 = α2,8) in the oligosaccharides of various glycoproteins. Thus, the reduced reactivity of MAL-I with mHSP60 after neuraminidase treatment confirmed the presence of α2, 3-linked sialic acid in the oligosaccharide portion of this glycoprotein.

To substantiate our finding regarding the sialoglycoprotein nature of mHSP60, the localization of this

glycoprotein along with their sialylation status in both subtypes of NSCLC cell lines was assessed under confocal microscope by fluorescence-based dual staining, using specific antibody against HSP60 and biotinylated MAL-I as the primary probes. A similar strategy was used by Rambaruth et al. (2012) to prove the glycan specific binding of *Helix pomatia* agglutinin (HPA) to integrin α6. Our findings have revealed the distribution of α2, 3 linked sialic acid containing HSP60 mainly on the membrane of both the cell lines, which was more prominent in the case of NCI-H520 cells. Our observations were further validated by immunohistochemical analysis of the adenocarcinoma and squamous cell carcinoma tissue sections, which showed prominent membrane positivity in the presence of HSP60-antibody and the extent of immunoreactivity in the case of adenocarcinoma tissue sections was more in comparison to the squamous cell carcinoma tissue sections.

Previously, we reported that MAA could induce distinct morphological changes as well as apoptosis in NSCLC cell lines (Mehta et al., 2013). As HSP60 is a MAA/MAL-I interacting membrane sialoglycoprotein of NSCLC cells and the antibody against HSP60 could appreciably inhibit MAL-I-induced morphological alteration in two major subtypes of NSCLC cell lines, as the antibody-binding site and MAL-I binding site in mHSP60 may be overlapping. Uncontrolled proliferation is one of the characteristics of cancer cells and the role of aberrant sialylation in the proliferation of cancer cells is well-established (Ma et al., 2016). The findings of our present study have clearly revealed the involvement of sialylated mHSP60 in the proliferation of both the subtypes of NSCLC cell lines, as the specific antibody against HSP60 could significantly inhibit the proliferation of these cells. The metastatic cascade is a complex process, comprising the movement of tumor cells away from the primary site of the tumor, their invasion into the bloodstream or lymphatic system, passage via-circulation, evasion at secondary tissues site and the formation of distant metastatic tumor colonies (van Zijl et al., 2011). It was observed that sialylation has significant impact on the functionality of integrins and ECM protein (e.g. fibronectin) involved in cell migration (Schultz et al., 2012). Thus, in this study the functional role of sialylated mHSP60 was assessed in view of migration of both subtypes of NSCLC cell lines. Our findings clearly indicated the involvement of sialylated mHSP60 in the migration of both the NSCLC cell lines, as this process could be inhibited in the presence of HSP60-antibody. In this context, it can be mentioned that annexin-II and HSP60 have been reported as the important future biomarkers for NSCLC, which may have a decisive role in assessment of metastatic potential, response to cure and in the establishment of differential diagnosis for adenocarcinoma and squamous cell carcinoma patients (Agababaoglu et al., 2017).

Taken together, our findings have suggested that α2,3 sialylated HSP60 may be a disease associated membrane-sialoglycoprotein in the case of NSCLC. As, sialylation and the progression of cancer is a correlated fact, it is possible that α2,3 sialylation might mediate the conformational alteration of mHSP60, involved in the proliferation and migration of the two major subtypes of NSCLC cell lines, indicating a probable role of sialylated mHSP60 in the disease process. All these findings have suggested the potential of the sialylated mHSP60 to be used as a target for the development of clinically useful strategies of better diagnostic and therapeutic potential for NSCLC.

Material and methods

Cell lines

A549 and NCI-H520 (Human NSCLC cell lines), obtained from NCCS (Pune, India), were propagated in RPMI 1640 medium supplemented with 10 mM HEPES (pH 7.4)/L-glutamine (2 mM)/sodium bicarbonate (1.5 g/l)/glucose(4.5 g/l)/sodium pyruvate (1 mM)/penicillin (50 U/ml)/streptomycin (50 μg/ml)/10% fetal bovine serum (FBS) (Thermo Fisher Scientific, Waltham, MA, USA).

Detection of MAL-I interacting membrane proteins of NSCLC cell lines

The membrane proteins of the two subtypes of NSCLC cell lines were isolated (Adamo et al., 1992) and the proteins were estimated using an RC-DC Kit (Bio-Rad, Hercules, CA, USA). The reactivity of MAL-I with the membrane fractions of each NSCLC cell line was assessed by a lectin overlay enzyme-linked assay using biotinylated MAL-I (Vector laboratory, Burlingame, CA, USA) as the primary probe. Briefly, a 96-well flat-bottomed enzyme immunoassay plate (Nunc, Roskilde, Denmark) was coated overnight with membrane fraction (protein content: 50 μg/ml) of each cell type in 50 mM carbonate/bicarbonate buffer (pH 9.6). Each well was washed with Tris-buffered saline (TBS) [20 mM TRIS hydrochloride (Tris/HCl) (pH 7.2)/150 mM sodium chloride (NaCl)] and treated (37°C, 2 h) with TBS 0.1% Tween 20 ($TBST_{0.5\%}$) [125 mM Tris/HCl (pH 7.5)/150 mM NaCl/0.5%Tween-20] to block the residual binding sites. Subsequently, each well of the plate was incubated (37°C, 2 h) with biotinylated MAL-I (2.5 μg/ml), washed with $TBST_{0.01\%}$ and treated (37°C, 1 h) with Streptavidin-Horse Radish Peroxidase (HRP) (1:5000; S911; Thermo Fisher Scientific, Waltham, MA, USA). After washing, the color was developed with 0.05% orthophenylenediamine in 0.15 M citrate/phosphate buffer (pH 5.0)/1 μl/

ml hydrogen peroxide. The reaction was stopped by the addition of 2 N sulfuric acid (H_2SO_4) to each well and quantitated in an enzyme-linked immunosorbent assay (ELISA) reader (Bio-Rad, Hercules, CA, USA) at 490 nm. Cells without biotinylated MAL-I (controls) were run in parallel.

MAL-I interacting membrane proteins of the cells were detected in lectin overlay transblots following 2D-PAGE (O'Farrell, 1975) of the membrane proteins isolated by the method of Adamo et al. (1992) as well as by using Mem-PER™ kit (Pierce, Rockford, IL, USA) as per the manufacturer's instructions. Briefly, after electrophoretic transfer of the proteins (Towbin et al., 1979) to the nitrocellulose membranes (GE Healthcare, Chicago, IL, USA), the membranes were placed in $TBST_{0.5\%}$ overnight at 4°C, washed and incubated (37°C, 2 h) with biotinylated MAL-I (1.3 µg/ml). After washing, the membranes were treated with Streptavidin-HRP (1:15 000; 37°C, 1 h). Finally, the membranes containing protein spots were developed using Super Signal® West Pico Chemiluminiscence Substrate (Thermo Fisher Scientific, Waltham, MA, USA) and photographed in Fluor-Chem M system (Protein Simple, San Jose, CA, USA). The M_r and the pI of the proteins of interest (Figure 2B) were determined from the plot of relative electrophoretic mobility (R_f) of the markers against their respective molecular weight and the plot of pI of the markers against their respective distance from the anode, respectively.

Identification of the proteins

MAL-I interacting membrane proteins of NSCLC cells were identified by MALDI-TOF-MS analysis (Shevchenko et al., 1996). Briefly, membrane proteins of each cell line were subjected to 2D-PAGE. After staining the gels with a MALDI compatible silver staining kit (Sigma-Aldrich, St. Louis, MO, USA), each gel slice containing the stained MAL-I interacting protein spot was destained and washed. This was followed by dehydration with acetonitrile and digestion with trypsin [Trypsin Singles, Proteomics Grade (Sigma-Aldrich, St. Louis, MO, USA); 20 µl (20 µg/ml as per manufacturer's instructions)], incubated at 37°C in a water bath overnight. After centrifugation, the supernatant containing peptides was collected and 0.1% trifluoroacetic acid (TFA) was added to each sample. Subsequently, each supernatant (1 µl) was mixed with 1 µl of the matrix solution [α-Cyano-4-hydroxycinnamic acid (Bruker Daltonics, Billerica, MA, USA), 10 mg/ml prepared in 50% acetonitrile (ACN)/0.1% TFA (aqueous)] and spotted (1 µl) separately on the grids of ground steel target plate (600/384F, Bruker Daltonics, Billerica, MA, USA) following the dried-droplet method (Kumarathasan et al., 2005). For the best possible calibration and mass accuracy enhancement a Peptide Calibration Standard II (Bruker Daltonics, Billerica, MA, USA) with the matrix solution was spotted adjacent to the samples. The PMF of each in-gel digested sample was obtained using MALDI-TOF-MS (Bruker Daltonics, Billerica, MA, USA) and matched against the MSDB database (Matrix Sciences) to identify MAL-I interacting membrane proteins. The identification of the selected protein was further substantiated by MS/MS analysis.

Confirmation of the identified protein

Western immunoblotting of membrane proteins of each cell line was performed to confirm the presence of the identified protein of interest, using the commercially available specific antibody against the selected identified protein as the primary probe. Briefly, after transferring the proteins (Towbin et al., 1979) to Hybond-ECL membranes following SDS-PAGE (Laemmli, 1970), the membranes were incubated in TBS containing 5% skimmed milk ($SM_{5\%}$-TBS) for 2 h at 37°C and treated with the primary antibody (at a required dilution). After washing, membranes were incubated in HRP-conjugated secondary antibody (at a required dilution). The membranes were washed and the protein bands on the membranes were developed with enhanced chemiluminiscence as mentioned earlier.

Characterization of the identified protein

The reactivity of the membrane protein with MAL-I was assessed in a lectin overlay transblot using biotinylated MAL-I (primary probe), as mentioned earlier. To check the carbohydrate specific interaction of MAL-I with the identified protein, MAL-I overlay transblotting was done in the presence of the specific inhibitor of the lectin. Briefly, after transferring the membrane proteins, the ECL-membranes were placed in $TBST_{0.5\%}$ overnight at 4°C, washed and treated with biotinylated MAL-I (1.3 µg/ml), pre-incubated (37°C for 3 h) with GM_2 [0.4 µg/ml (Sigma-Aldrich, St. Louis, MO, USA); a specific inhibitor of MAA (Kapoor et al., 2008)/MAL-I. After washing, membranes were treated with streptavidin-HRP (1:15 000; 37°C, 1 h). Finally, the protein was developed as mentioned earlier. Characterization of the identified protein was also done by enzymatic deglycosylation (Hino et al., 2003) using Neuraminidase (Sigma-Aldrich, St. Louis, MO, USA), O-glycanase and N-glycanase (Boehringer Mannheim, USA) separately followed by its interaction with MAL-I. For this, the membrane proteins were transferred to nitrocellulose membranes following SDS-PAGE. Proteins on the trans-blots were treated with Neuraminidase (2 U/ml) in 10 mM TBS (pH 6.5). For O- and N-glycanase treatment, the proteins on the membranes were incubated (24 h, 37°C) with O-glycanase (10 mU/ml) and N-glycanase (5 mU/ml) separately in 66 mM sodium acetate buffer (pH 5.0)/1.3 mM $CaCl_2$. Subsequently, the protein band was developed using biotinylated MAL-I as the primary probe and the intensity of the band was analyzed using ImageJ software (National Institutes of Health, Bethesda, MD, USA).

Further, MAL-I reactivity and thus the sialoglycoprotein nature of the identified membrane protein on the two major subtypes of NSCLC cell lines was assessed by fluorescence-based dual staining. Briefly, the cells (7×10^4) grown on cover slips in 24-well plates (500 µl medium/well) were washed 3 times in PBS followed by fixation for 20 min in 4% paraformaldehyde in PBS. The residual binding sites were blocked by 1% desialylated-BSA (prepared by incubation of 1% BSA solution in 50 mM H_2SO_4 at 80°C for 2 h followed by dialysis against distilled water) at 37°C for 1 h in a moistened chamber. Cells were kept overnight at 4°C with antibody (at a required dilution) against the identified protein. After washing, the cells were incubated with biotinylated MAL-I (2.5 µg/ml) at 37°C for 3 h. After washing, FITC-labeled secondary antibody (at a required dilution) and Texas-Red labeled-Streptavidin (1:100; RPN1233V, Amersham Biosciences, UK) were added simultaneously. Following incubation (2 h, 37°C), the cells were washed and stained with diamidino-2-phenylindole (DAPI, 0.1%) for 2–3 min. After extensive washing, the cover slips with the stained cells were kept on slides with glycerol for proper mounting and the cells were observed under confocal microscope (Olympus-IX81, Fluoview).

Validation of the identified protein on the tissue samples

Immunohistochemical analysis was done to assess the presence of the identified protein in the tissue sections of biopsy samples from NSCLC patients [adenocarcinoma patients (n = 8), squamous cell carcinoma patients (n = 6)] and adjacent normal lung biopsy samples, obtained from the Department of Histopathology (PGIMER, Chandigarh, India). Sections (4 µm) obtained from each biopsy sample were taken on coated slides (poly-L-lysine). Then, the sections were deparaffinized in xylene, hydrated with a series of graded ethanol and kept in tri-sodium citrate buffer (pH 6.0) for antigen retrieval. Subsequently, for removal of endogenous peroxidase, sections were incubated in 0.3% H_2O_2/methanol for 20 min, followed by the addition of the antibody (at a required dilution) against the identified protein. Further, the sections were washed with PBS and incubated in HRP conjugated secondary antibody (at a required dilution). Finally, the sections were developed with 0.05% 3,3′-diaminobenzidine tetrahydrochloride/1 µl/ml H_2O_2 and stained with hematoxylin. The H-score analysis was done using GraphPad Prism 6.0.

Functional characterization of the identified protein

Morphological alteration

The role of the identified protein on MAL-I induced morphological alteration of the two major subtypes of NSCLC cell lines was assessed. Briefly, cells (5×10^4/500 µl media/well) were seeded in 24-well cell culture plates (Greiner Bio-One, Germany) at 37°C and grown up to 70–80% confluency. Furthermore, cells were treated with MAL-I (0.5 µg/ml and 1 µg/ml in case of NCI-H520 and A549 cells, respectively) in the absence and presence of the antibody (at a required dilution) against the identified protein for 24 h at 37°C. The morphological changes in the cells were observed under an inverted microscope.

Cell proliferation assay

Cell proliferation assay was done using the method of Mosmann (1983). Briefly, 5×10^3 cells were inoculated in 200 µl RPMI 1640 media/10% FBS into the wells of 96-well plates (Greiner Bio-One, Germany) and incubated until 85–90% confluency at 37°C. After washing, the cells were cultured for 48 h in RPMI 1640 media/FBS (0.2%) with and without the antibody (at a required dilution) the against the identified protein. This was followed by the addition of 10 µl of MTT (5 mg/ml, Sigma-Aldrich, St. Louis, MO, USA) to each well 4 h before the completion of the incubation period. After removal of the medium, DMSO (100 µl) was added to dissolve the formazan crystals formed by the viable cells in each well. The optical density of each well was noted at 570 nm in Multimode Microplate Reader (Infinite M200 PRO Tecan Life Science, Switzerland).

Cell migration assay

The method of Cai et al. (2010) was followed to assess the role of the identified protein on migration of NSCLC cells. Briefly, the cells (5×10^4/500 µl media/well) were seeded into the wells of the 24-well plates and incubated at 37°C till 85–90% confluency. A scratch was made through the confluent monolayer using a sterile tip (P200 pipette tip). The cells were washed and cultured in RPMI 1640 media/FBS (0.2%) in the absence and presence of the antibody (at a required dilution) against the identified protein. The cells were incubated for different time intervals to assess cell migration. The images of the cells that migrated into the scratched area of the wells were captured at 12-h interval under an inverted microscope. Markings were created to obtain the same field during the image acquisition. Analysis was performed using T-scratch [CSE Lab, Zurich; Geback et al. (2009)] software to calculate the percentage of the area filled at different time intervals. Each set of the experiment was performed twice in triplicates.

Statistical analysis

Data were analyzed by using analysis of variance (ANOVA) and an unpaired '*t*' test as per need.

Acknowledgments: A grant [no. 27 (0261)/12/EMR-II] from the Council of Scientific and Industrial Research (CSIR), New Delhi, India, supported this work.

Conflict of interest statement: The authors declare no conflict of interests.

References

Abdalla, M.A. and Haj-Ahmad, Y. (2012). Promising urinary protein biomarkers for the early detection of hepatocellular carcinoma among high-risk hepatitis C virus egyptian patients. J. Cancer *3*, 390–403.

Adamo, H.P., Verma, A.K., Sanders, M.A., Heim, R., Salisbury, J.L., Wieben, E.D., and Penniston, J.T. (1992). Overexpression of the erythrocyte plasma membrane Ca^{2+} pump in COS-1 cells. Biochem. J. *285*, 791–797.

Agababaoglu, I., Onen, A., Demir, A.B., Aktas, S., Altun, Z., Ersoz, H., Sanl, A., Ozdemir, N., and Akkoclu, A. (2017). Chaperonin (HSP60) and annexin-2 are candidate biomarkers for non-small cell lung carcinoma. Medicine *96*, e5903.

Babal, P., Janega, P., Cerna, A., Kholova, I., and Brabencova, E. (2006). Neoplastic transformation of the thyroid gland is accompanied by changes in cellular sialylation. Acta Histochem. *108*, 133–140.

Bodzek, P., Partyka, R., and Damasiewicz-Bodzek, A. (2014). Antibodies against Hsp60 and Hsp65 in the sera of women with ovarian cancer. J. Ovarian Res. *7*, 30.

Bray, F., Ferlay, J., Soerjomataram, I., Siegel, R.L., Torre, L.A., and Jemal, A. (2018). Global cancer statistics 2018: GLOBOCAN estimates of incidence and mortality worldwide for 36 cancers in 185 countries. CA Cancer J. Clin. *68*, 394–424.

Cai, Z., Wang, Q., Zhou, Y., Zheng, L., Chiu, J.F., and He, Q.Y. (2010). Epidermal growth factor-induced epithelial-mesenchymal transition in human esophageal carcinoma cells – a model for the study of metastasis. Cancer Lett. *296*, 88–95.

Campanella, C., Bucchieri, F., Merendino, A.M., Fucarino, A., Burgio, G., Corona, D.F., Barbieri, G., David, S., Farina, F., Zummo, G., et al. (2012). The odyssey of Hsp60 from tumor cells to other destinations includes plasma membrane-associated stages and Golgi and exosomal protein-trafficking modalities. PLoS One *7*, e42008.

Cao, Y., Liang, H., Zhang, F., Luan, Z., Zhao, S., Wang, X.A., Liu, S., Bao, R., Shu, Y., Ma, Q., et al. (2016). Prohibitin overexpression predicts poor prognosis and promotes cell proliferation and

invasion through ERK pathway activation in gallbladder cancer. J. Exp. Clin. Cancer Res. *35*, 68.

Cappello, F., Bellafiore, M., Palma, A., David, S., MarcianÃ, V., Bartolotta, T., SciumÃ, C., Modica, G., Farina, F., and Zummo, G. (2009). 60KDa chaperonin (HSP60) is over-expressed during colorectal carcinogenesis. Eur. J. Histochem. *47*, 105–110.

Castilla, C., Congregado, B., Conde, J.M., Medina, R., Torrubia, F.J., Japon, M.A., and Saez, C. (2010). Immunohistochemical expression of Hsp60 correlates with tumor progression and hormone resistance in prostate cancer. Urology *76*, 1017.e1011–1016.

Cawthorn, T.R., Moreno, J.C., Dharsee, M., Tran-Thanh, D., Ackloo, S., Zhu, P.H., Sardana, G., Chen, J., Kupchak, P., Jacks, L.M., et al. (2012). Proteomic analyses reveal high expression of decorin and endoplasmin (HSP90B1) are associated with breast cancer metastasis and decreased survival. PLoS One *7*, e30992.

Chaiwatanasirikul, K. and Sala, A. (2011). The tumour-suppressive function of CLU is explained by its localisation and interaction with HSP60. Cell Death Dis. *2*, e219.

Chauhan, J.S., Rao, A., and Raghava, G.P. (2013). In silico platform for prediction of N-, O- and C-glycosites in eukaryotic protein sequences. PLoS One *8*, e67008.

Cummings, R.D., Darvill, A.G., Etzler, M.E., and Hahn, M.G. (2015). Glycan-recognizing probes as tools. In: Essentials of Glycobiology (NY: Cold Spring Harbor), pp. 611–625.

Desmetz, C., Bibeau, F., Boissiere, F., Bellet, V., Rouanet, P., Maudelonde, T., Mange, A., and Solassol, J. (2008). Proteomics-based identification of HSP60 as a tumor-associated antigen in early stage breast cancer and ductal carcinoma in situ. J. Proteome. Res. *7*, 3830–3837.

Geback, T., Schulz, M.M., Koumoutsakos, P., and Detmar, M. (2009). TScratch: a novel and simple software tool for automated analysis of monolayer wound healing assays. Biotechniques *46*, 265–274.

Giaginis, C., Daskalopoulou, S.S., Vgenopoulou, S., Sfiniadakis, I., Kouraklis, G., and Theocharis, S.E. (2009). Heat Shock Protein-27, -60 and -90 expression in gastric cancer: association with clinicopathological variables and patient survival. BMC Gastroenterol. *9*, 14.

Giarnieri, E., De Francesco, G.P., Carico, E., Midiri, G., Amanti, C., Giacomelli, L., Tucci, G., Gidaro, S., Stroppa, I., Gidaro, G., et al. (2005). Alpha- and beta-tubulin expression in rectal cancer development. Anticancer Res. *25*, 3237–3241.

Goplen, D., Wang, J., Enger, P.O., Tysnes, B.B., Terzis, A.J., Laerum, O.D., and Bjerkvig, R. (2006). Protein disulfide isomerase expression is related to the invasive properties of malignant glioma. Cancer Res. *66*, 9895–9902.

Hamrita, B., Chahed, K., Kabbage, M., Guillier, C.L., Trimeche, M., Chaieb, A., and Chouchane, L. (2008). Identification of tumor antigens that elicit a humoral immune response in breast cancer patients' sera by serological proteome analysis (SERPA). Clin. Chim. Acta *393*, 95–102.

Hauselmann, I. and Borsig, L. (2014). Altered tumor-cell glycosylation promotes metastasis. Front Oncol. *4*, 28.

Hayoun, D., Kapp, T., Edri-Brami, M., Ventura, T., Cohen, M., Avidan, A., and Lichtenstein, R.G. (2012). HSP60 is transported through the secretory pathway of 3-MCA-induced fibrosarcoma tumour cells and undergoes N-glycosylation. FEBS J. *279*, 2083–2095.

Hino, M., Kijima-Suda, I., Nagai, Y., and Hosoya, H. (2003). Glycosylation of the α and β tubulin by sialyloligosaccharides. Zoolog. Sci. *20*, 709–715.

Hjerpe, E., Egyhazi, S., Carlson, J., Stolt, M.F., Schedvins, K., Johansson, H., Shoshan, M., and Åvall-Lundqvist, E. (2013). HSP60 predicts survival in advanced serous ovarian cancer. Int. J. Gynecol. Cancer *23*, 448–455.

Hou, J., Li, X., Li, C., Sun, L., Zhao, Y., Zhao, J., and Meng, S. (2015). Plasma membrane gp96 enhances invasion and metastatic potential of liver cancer via regulation of uPAR. Mol. Oncol. *9*, 1312–1323.

Hwang, Y.J., Lee, S.P., Kim, S.Y., Choi, Y.H., Kim, M.J., Lee, C.H., Lee, J.Y., and Kim, D.Y. (2009). Expression of heat shock protein 60 kDa is upregulated in cervical cancer. Yonsei Med. J. *50*, 399–406.

Inagaki, Y., Tang, W., Guo, Q., Kokudo, N., Sugawara, Y., Karako, H., Konishi, T., Nakata, M., Nagawa, H., and Makuuchi, M. (2007). Sialoglycoconjugate expression in primary colorectal cancer and metastatic lymph node tissues. Hepatogastroenterology *54*, 53–57.

Inagaki, Y., Usuda, M., Xu, H., Wang, F., Cui, S., Mafune, K., Sugawara, Y., Kokudo, N., Tang, W., and Nakata, M. (2008). Appearance of high-molecular weight sialoglycoproteins recognized by Maackia amurensis leukoagglutinin in gastric cancer tissues: a case report using 2-DE-lectin binding analysis. Biosci. Trends *2*, 151–154.

Isaji, T., Im, S., Kameyama, A., Wang, Y., Fukuda, T., and Gu, J. (2019). A complex between phosphatidylinositol 4 kinase IIα and integrin $\alpha 3\beta 1$ is required for N-glycan sialylation in cancer cells. J. Biol. Chem. *294*, RA118. 005208.

Izdebska, M., Zielinska, W., Grzanka, D., and Gagat, M. (2018). the role of actin dynamics and actin-binding proteins expression in epithelial-to-mesenchymal transition and its association with cancer progression and evaluation of possible therapeutic targets. Biomed. Res. Int. *2018*, 4578373.

Kamath, A., Joseph, A.M., Gupta, K., Behera, D., Jaiswal, A., Dewan, R., and Rajala, M.S. (2015). Proteomic analysis of HEK293 cells expressing non small cell lung carcinoma associated epidermal growth factor receptor variants reveals induction of heat shock response. Exp. Hematol. Oncol. *4*, 1.

Kapoor, S., Marwaha, R., Majumdar, S., and Ghosh, S. (2008). Apoptosis induction by Maackia amurensis agglutinin in childhood acute lymphoblastic leukemic cells. Leuk. Res. *32*, 559–567.

Kawaguchi, T., Matsumoto, I., and Osawa, T. (1974). Studies on hemagglutinins from *Maackia amurensis* seeds. J. Biol. Chem. *249*, 2786–2792.

Khan, I.U., Wallin, R., Gupta, R.S., and Kammer, G.M. (1998). Protein kinase A-catalyzed phosphorylation of heat shock protein 60 chaperone regulates its attachment to histone 2B in the T lymphocyte plasma membrane. Proc. Natl. Acad. Sci. U.S.A. *95*, 10425–10430.

Kumarathasan, P., Mohottalage, S., Goegan, P., and Vincent, R. (2005). An optimized protein in-gel digest method for reliable proteome characterization by MALDI-TOF-MS analysis. Anal. Biochem. *346*, 85–89.

Laemmli, U.K. (1970). Cleavage of structural proteins during the assembly of the head of bacteriophage T4. Nature *227*, 680–685.

Lalli, R.C., Kaur, K., Dadsena, S., Chakraborti, A., Srinivasan, R., and Ghosh, S. (2015). Maackia amurensis agglutinin enhances paclitaxel induced cytotoxicity in cultured non-small cell lung cancer cells. Biochimie *115*, 93–107.

Lalli, R., Kaur, K., Chakraborti, A., Srinivasan, R., and Ghosh, S. (2019). *Maackia amurensis* agglutinin induces apoptosis in

cultured drug resistant human non-small cell lung cancer cells. Glycoconj J. *36*, 473–485.

Linxweiler, J., Kollipara, L., Zahedi, R.P., Lampel, P., Zimmermann, R., and Greiner, M. (2014). Proteomic insights into non-small cell lung cancer: New ideas for cancer diagnosis and therapy from a functional viewpoint. EuPA Open Proteom. *4*, 25–39.

Lopez-Morales, D., Reyes-Leyva, J., Santos-Lopez, G., Zenteno, E., and Vallejo-Ruiz, V. (2010). Increased expression of sialic acid in cervical biopsies with squamous intraepithelial lesions. Diagn Pathol. *5*, 74.

Luan, Z., He, Y., Alattar, M., Chen, Z., and He, F. (2014). Targeting the prohibitin scaffold-CRAF kinase interaction in RAS-ERK-driven pancreatic ductal adenocarcinoma. Mol. Cancer *13*, 38.

Ma, X., Dong, W., Su, Z., Zhao, L., Miao, Y., Li, N., Zhou, H., and Jia, L. (2016). Functional roles of sialylation in breast cancer progression through miR-26a/26b targeting ST8SIA4. Cell Death Dis. *7*, e2561.

MacArthur, I.C., Bei, Y., Garcia, H.D., Ortiz, M.V., Toedling, J., Klironomos, F., Rolff, J., Eggert, A., Schulte, J.H., Kentsis, A., et al. (2019). Prohibitin promotes de-differentiation and is a potential therapeutic target in neuroblastoma. JCI Insight *5*.

Marzec, M., Eletto, D., and Argon, Y. (2012). GRP94: An HSP90-like protein specialized for protein folding and quality control in the endoplasmic reticulum. Biochim. Biophys. Acta *1823*, 774–787.

Matsuda, Y., Ishiwata, T., Yoshimura, H., Hagio, M., and Arai, T. (2015). Inhibition of nestin suppresses stem cell phenotype of glioblastomas through the alteration of post-translational modification of heat shock protein HSPA8/HSC71. Cancer Lett. *357*, 602–611.

Mehta, S., Chhetra, R., Srinivasan, R., Sharma, S.C., Behera, D., and Ghosh, S. (2010). Detection of disease specific sialoglycoconjugate specific antibodies in bronchoalveolar lavage fluid of non-small cell lung cancer patients. Glycoconj. J. *27*, 491–500.

Mehta, S., Chhetra, R., Srinivasan, R., Sharma, S.C., Behera, D., and Ghosh, S. (2013). Potential importance of Maackia amurensis agglutinin in non-small cell lung cancer. Biol. Chem. *394*, 889–900.

Merendino, A.M., Bucchieri, F., Campanella, C., Marciano, V., Ribbene, A., David, S., Zummo, G., Burgio, G., Corona, D.F., Conway de Macario, E., et al. (2010). Hsp60 is actively secreted by human tumor cells. PLoS One *5*, e9247.

Morales, C., Wu, S., Yang, Y., Hao, B., and Li, Z. (2009). Drosophila glycoprotein 93 Is an ortholog of mammalian heat shock protein gp96 (grp94, HSP90b1, HSPC4) and retains disulfide bond-independent chaperone function for TLRs and integrins. J. Immunol. *183*, 5121–5128.

Mosmann, T. (1983). Rapid colorimetric assay for cellular growth and survival: application to proliferation and cytotoxicity assays. J. Immunol. Methods *65*, 55–63.

Munkley, J. and Scott, E. (2019). Targeting aberrant sialylation to treat cancer. Medicines (Basel) *6*.

O'Farrell, P.H. (1975). High resolution two-dimensional electrophoresis of proteins. J. Biol. Chem. *250*, 4007–4021.

Ochoa-Alvarez, J.A., Krishnan, H., Shen, Y., Acharya, N.K., Han, M., McNulty, D.E., Hasegawa, H., Hyodo, T., Senga, T., Geng, J.G., et al. (2012). Plant lectin can target receptors containing sialic acid, exemplified by podoplanin, to inhibit transformed cell growth and migration. PLoS One *7*, e41845.

Ohyama, C., Hosono, M., Nitta, K., Oh-eda, M., Yoshikawa, K., Habuchi, T., Arai, Y., and Fukuda, M. (2004). Carbohydrate structure and differential binding of prostate specific antigen to Maackia amurensis lectin between prostate cancer and benign prostate hypertrophy. Glycobiology *14*, 671–679.

Okamoto, T., Yamamoto, H., Kudo, I., Matsumoto, K., Odaka, M., Grave, E., and Itoh, H. (2017). HSP60 possesses a GTPase activity and mediates protein folding with HSP10. Sci. Rep. *7*, 16931.

Oser, M.G., Niederst, M.J., Sequist, L.V., and Engelman, J.A. (2015). Transformation from non-small-cell lung cancer to small-cell lung cancer: molecular drivers and cells of origin. Lancet Oncol. *16*, e165–172.

Parikh, P.M., Ranade, A.A., Govind, B., Ghadyalpatil, N., Singh, R., Bharath, R., Bhattacharyya, G.S., Koyande, S., Singhal, M., Vora, A., et al. (2016). Lung cancer in India: Current status and promising strategies. South Asian J. Cancer *5*, 93–95.

Patel, V., Hood, B.L., Molinolo, A.A., Lee, N.H., Conrads, T.P., Braisted, J.C., Krizman, D.B., Veenstra, T.D., and Gutkind, J.S. (2008). Proteomic analysis of laser-captured paraffin-embedded tissues: a molecular portrait of head and neck cancer progression. Clin. Cancer Res. *14*, 1002–1014.

Pearson, A.J. and Gallagher, E.S. (2019). Overview of characterizing cancer glycans with lectin-based analytical methods. Methods Mol. Biol. *1928*, 389–408.

Rambaruth, N.D., Greenwell, P., and Dwek, M.V. (2012). The lectin Helix pomatia agglutinin recognizes O-GlcNAc containing glycoproteins in human breast cancer. Glycobiology *22*, 839–848.

Ribeiro, A.C., Ferreira, R., and Freitas, R. (2018). Chapter 1 – plant lectins: bioactivities and bioapplications. In: Studies in Natural Products Chemistry. (Elsevier), pp. 1–42.

Schultz, M.J., Swindall, A.F., and Bellis, S.L. (2012). Regulation of the metastatic cell phenotype by sialylated glycans. Cancer Metastasis Rev. *31*, 501–518.

Shevchenko, A., Wilm, M., Vorm, O., and Mann, M. (1996). Mass spectrometric sequencing of proteins silver-stained polyacrylamide gels. Anal. Chem. *68*, 850–858.

Silva, M.L.S. (2018). Lectin-based biosensors as analytical tools for clinical oncology. Cancer Lett. *436*, 63–74.

Singh, S.S., Wong, J.H., Ng, T.B., Singh, W.S., and Thangjam, R. (2019). Biomedical Applications of Lectins from Traditional Chinese Medicine. Curr Protein Pept Sci. *20*, 220–230.

Sun, L., Guo, C., Cao, J., Burnett, J., Yang, Z., Ran, Y., and Sun, D. (2017). Over-expression of alpha-enolase as a prognostic biomarker in patients with pancreatic cancer. Int J Med Sci. *14*, 655–661.

Syed, P., Gidwani, K., Kekki, H., Leivo, J., Pettersson, K., and Lamminmaki, U. (2016). Role of lectin microarrays in cancer diagnosis. Proteomics *16*, 1257–1265.

Takashima, M., Kuramitsu, Y., Yokoyama, Y., Iizuka, N., Toda, T., Sakaida, I., Okita, K., Oka, M., and Nakamura, K. (2003). Proteomic profiling of heat shock protein 70 family members as biomarkers for hepatitis C virus-related hepatocellular carcinoma. Proteomics *3*, 2487–2493.

Tang, W., Guo, Q., Usuda, M., Kokudo, N., Seyama, Y., Minagawa, M., Sugawara, Y., Nakata, M., Kojima, N., and Makuuchi, M. (2005). Histochemical expression of sialoglycoconjugates in carcinoma of the papilla of Vater. Hepatogastroenterology *52*, 67–71.

Towbin, H., Staehelin, T., and Gordon, J. (1979). Electrophoretic transfer of proteins from polyacrylamide gels to nitrocellulose sheets: procedure and some applications. Proc. Natl. Acad. Sci. U.S.A. *76*, 4350–4354.

Tsai, Y.P., Yang, M.H., Huang, C.H., Chang, S.Y., Chen, P.M., Liu, C.J., Teng, S.C., and Wu, K.J. (2009). Interaction between HSP60 and beta-catenin promotes metastasis. Carcinogenesis *30*, 1049–1057.

Tufo, G., Jones, A.W., Wang, Z., Hamelin, J., Tajeddine, N., Esposti, D.D., Martel, C., Boursier, C., Gallerne, C., Migdal, C., et al. (2014). The protein disulfide isomerases PDIA4 and PDIA6 mediate resistance to cisplatin-induced cell death in lung adenocarcinoma. Cell Death Differ. *21*, 685–695.

van Zijl, F., Krupitza, G., and Mikulits, W. (2011). Initial steps of metastasis: cell invasion and endothelial transmigration. Mutat. Res. *728*, 23–34.

Wang, W.-C. and Cummings, R. (1988). The immobilized leukoagglutinin from the seeds of Maackia amurensis binds with high affinity to complex-type Asn-linked oligosaccharides containing terminal sialic acid-linked α-2,3 to penultimate galactose residues. J. Biol. Chem. *263*, 4576–4585.

Wang, Q., He, Z., Zhang, J., Wang, Y., Wang, T., Tong, S., Wang, L., Wang, S., and Chen, Y. (2005). Overexpression of endoplasmic reticulum molecular chaperone GRP94 and GRP78 in human lung cancer tissues and its significance. Cancer Detect. Prev. *29*, 544–551.

Wu, J., Liu, T., Rios, Z., Mei, Q., Lin, X., and Cao, S. (2017). Heat shock proteins and cancer. Trends Pharmacol. Sci. *38*, 226–256.

Xu, Y.X.Z., Bassi, G., and Mishra, S. (2019). Prohibitin: a prime candidate for a pleiotropic effector that mediates sex differences in obesity, insulin resistance, and metabolic dysregulation. Biol. Sex Differ. *10*, 25.

Yao, X., Liu, H., Zhang, X., Zhang, L., Li, X., Wang, C., and Sun, S. (2015). Cell surface GRP78 accelerated breast cancer cell proliferation and migration by activating STAT3. PLoS One *10*, e0125634.

Yau, T., Dan, X., Ng, C.C., and Ng, T.B. (2015). Lectins with potential for anti-cancer therapy. Molecules *20*, 3791–3810.

Zhu, X., Xu, Y., Solis, L.M., Tao, W., Wang, L., Behrens, C., Xu, X., Zhao, L., Liu, D., Wu, J., et al. (2015). Long-circulating siRNA nanoparticles for validating Prohibitin1-targeted non-small cell lung cancer treatment. Proc. Natl. Acad. Sci. U.S.A. *112*, 7779–7784.